THE JOURNAL OF BIOLOGICAL CHEMISTRY VOL. 289, NO. 31, pp. 21673–21683, August 1, 2014

Forces and Dynamics of Glucose and Inhibitor Binding to Sodium Glucose Co-transporter SGLT1 Studied by Single Molecule Force Spectroscopy*

Received for publication, June 16, 2014 Published, JBC Papers in Press, June 24, 2014, DOI 10.1074/jbc.M113.529875

Isabel Neundlinger[‡1], Theeraporn Puntheeranurak[‡§1], Linda Wildling[‡], Christian Rankl[¶], Lai-Xi Wang[‖], Hermann J. Gruber[‡], Rolf K. H. Kinne[**], and Peter Hinterdorfer[‡2]

*From the [‡]Institute for Biophysics, Johannes Kepler University of Linz, Gruberstrasse 40, 4020 Linz, Austria, [§]Department of Biology, Faculty of Science, Mahidol University and Nanotec-MU Center of Excellence on Intelligent Materials and Systems, 272 Rama VI, Ratchathewi, Bangkok 10400, Thailand, [¶]Agilent Technologies, Gruberstrasse 40, 4020 Linz, Austria, [‖]Institute of Human Virology and Department of Biochemistry and Molecular Biology, University of Maryland School of Medicine, Baltimore, Maryland 21201, and **Max Planck Institute of Molecular Physiology, Otto-Hahn Strasse 11, 44227 Dortmund, Germany*

Background: SGLT1 functions in intestinal glucose absorption and renal reabsorption.
Results: With increasing temperature, width of energy barrier and average life time increased for glucose binding to SGLT1 but decreased for phlorizin binding.
Conclusion: Sugar translocation and inhibitor binding involves several steps with different temperature sensitivity.
Significance: Force spectroscopy can be used to study dynamics and structure of membrane transporter.

Single molecule force spectroscopy was employed to investigate the dynamics of the sodium glucose co-transporter (SGLT1) upon substrate and inhibitor binding on the single molecule level. CHO cells stably expressing rbSGLT1 were probed by using atomic force microscopy tips carrying either thioglucose, 2′-aminoethyl β-D-glucopyranoside, or aminophlorizin. Poly(ethylene glycol) (PEG) chains of different length and varying end groups were used as tether. Experiments were performed at 10, 25 and 37 °C to address different conformational states of SGLT1. Unbinding forces between ligands and SGLT1 were recorded at different loading rates by changing the retraction velocity, yielding binding probability, width of energy barrier of the binding pocket, and the kinetic off rate constant of the binding reaction. With increasing temperature, width of energy barrier and average life time increased for the interaction of SGLT1 with thioglucose (coupled via acrylamide to a long PEG) but decreased for aminophlorizin binding. The former indicates that in the membrane-bound SGLT1 the pathway to sugar translocation involves several steps with different temperature sensitivity. The latter suggests that also the aglucon binding sites for transport inhibitors have specific, temperature-sensitive conformations.

Glucose uptake into cells is essential for supply of energy in almost every organism from invertebrate to mammalian. The sugar can enter cells either by passive diffusion via facilitating transporters of the GLUT family or by secondary active transport via sodium-glucose co-transporters (SGLTs)[3] using the electrochemical Na^+ gradient across the cell membrane generated by Na^+/K-ATPase as the driving force (1–3). SGLT1 is a member of the large solute carrier family (SCL5) present in the apical membrane of the epithelial cells of the small intestine and the kidney and participating in intestinal glucose absorption and renal glucose reabsorption in many species (1). Mutations of SGLT1 can cause severe malfunctions such as glucose-galactose-malabsorption, a serious disease in newborn children in which they may die due to diarrhea and dehydration (4). Moreover, sodium-glucose co-transporters are therapeutic targets to treat hyperglycemia in type 2 diabetes (5, 6). Hence, a detailed elucidation of the structure and function of SGLT1 is required.

To this end various methods have been used such as kinetic studies (7), electrophysiology methods (8), tryptophan scanning studies (9, 10), mutagenesis studies (11, 12), x-ray crystallography (13), and plasmon resonance spectroscopy (14) to name a few. Crystallographic data are available for *Vibrio parahemeolyticus* sodium/galactose symporter (vSGLT) (13) in the sodium- and galactose-bound state. Overall, a group of seven central helices contributes side-chain interactions for ligand selectivity. These are stabilized by seven supporting helices. The model proposed recently by Sala-Rabanal *et al.* (15) integrates the kinetic and structural data available to date into a six-step alternating access model.

Our group has successfully used atomic force microscopy (AFM) and single molecule recognition force spectroscopy (16–18) to probe the transporter in its natural environment embedded in the plasma membrane of living cells under near-physiological conditions (19). The extracellular location and

* This work was supported by the State of Upper Austria and the Austrian Science Fund (Project SFB35) and supported in part by the Nanotechnology Center (NANOTEC), National Science and Technology Development Agency (NSTDA), Ministry of Science and Technology, Thailand, through its program of Center of Excellence Network.
[1] Both authors contributed equally to this work.
[2] To whom correspondence should be addressed. Tel.: 43-732-2468-7631; Fax: 43-732-2468-822; E-mail: peter.hinterdorfer@jku.at.

[3] The abbreviations used are: SGLT1, sodium glucose co-transporter I; AFM, atomic force microscopy; thio-glc, 1-thio-β-D-glucose; AcS-, acetylthio-; hex-glc, AcS-hexyl-glucose; hex-phl, AcS-aminophlorizin; NHS, *N*-hydroxysuccinimide; N, newtons; AA-PEG_{5000}, acrylamide-PEG-linker; BIC, Bayesian information criterion; mal-PEG_{1300}, maleimide-PEG_{1300}-NHS.

accessibility of three extramembraneous loops (loop 6–7, loop 8–9, and loop 13–14) was identified. They form a vestibule for the entry of the sugar into the translocation pathway and contain the first of several sugar recognition sites. This vestibule is accessible to the sugar only in the presence of sodium (20, 21). Phlorizin acts as a competitive inhibitor of SGLT1 with an apparent K_i of 1 μM (22). The phlorizin carrier complex represents a dead end conformation of the transporter in which it is locked into a condensed, rigid conformation unable to mediate translocation (23, 24). Phlorizin consists of a pyranose ring (sugar residue) and two aromatic rings joined by an alkyl spacer (the aglucon moiety, phloretin) (22). It is supposed that phlorizin binds via a two-step mechanism to the sugar translocation site and an aglucon binding site of the transporter (8, 25). One of the extracellular loops, loop 13–14, was found to provide an additional aglucon binding site. Alkyl-glucosides, such as hexyl-glucoside, also inhibit glucose transport competitively with a K_i of ~10 μM (26, 27). The sites of interaction between the aglucon of the inhibitors and loop 13–14 differ and overlap only partly (10).

In the present work AFM was employed to further characterize the molecular interaction between SGLT1 and D-glucose and inhibitors with regard to their dynamics and forces. Molecular interaction between receptors and ligands is controlled by a complex array of intermolecular forces that can be characterized by their free energy landscape. AFM can be used to directly quantify the range and magnitude of the interaction forces between proteins and other molecules (28, 29). Dynamic aspects of bond rupture, *e.g.* dissociation rate constants, commonly used to describe the affinity between a ligand and a protein, and width of energy barrier, interpreted as the distance of the energy barrier from the energy minimum along the direction of the applied force, can be obtained by varying the loading rate of the force appliance. This provides insights into the molecular dynamics and the energy landscape for substrate/inhibitor-transporter complexes. Location of energy barriers and nature of interaction forces have been studied extensively for proteins by investigating their properties at different temperatures (30). We used a similar approach as it has been shown that sodium-dependent glucose transport is strongly temperature-dependent (11), ceasing below the transition temperature of the membrane lipids *in vitro* (31). In contrast, sodium-dependent, glucose-inhibitable binding of phlorizin is still demonstrable at temperatures close to 0 °C.[4] Therefore, studies were performed at 10, 25, and 37 °C to investigate further the properties of the glucose translocation pathway and the inhibitor binding sites.

EXPERIMENTAL PROCEDURES

AFM Tip Functionalization—1-Thio-β-D-glucose (thio-glc) (Sigma), 2′-aminoethyl β-D-glucopyranoside, and 3-aminophlorizin were coupled to the AFM tip using a well established three-step protocol. Therefore, 2′-aminoethyl β-D-glucopyranoside was synthesized as described (32) and *N*-acylated with *N*-succinimidyl 6-(acetylthio)hexanoate as previously described for "tris-nitrilotriacetic acid" (33) yielding the product AcS-hex-glc. Immediately before coupling to the AFM tip, the acetyl group was removed with hydroxylamine (34) to obtain a free thiol, abbreviated as hex-glc (Fig. 1*A*). 3-Aminophlorizin was synthesized as described (35) except that sodium dithionite was used for reduction of 3-nitrophlorizin instead of catalytic hydrogenation (36). 3-Aminophlorizin was also extended with 6-(acetylthio)hexanoic acid, yielding a conjugate termed AcS-hex-phl. Immediately before coupling to the AFM tip, the acetyl group was removed with hydroxylamine (34) to obtain a free thiol. The molecule was abbreviated as hex-phl (Fig. 1*A*). Two different polyethylene glycol (PEG) spacers were used to couple the glucose derivatives to the tip. Maleimide-PEG_{1300}-NHS was purchased from Polypure (Oslo, Norway). Acrylamide-PEG_{5000}-NHS was synthesized by reacting NH_2-PEG_{5000}-COOH hydrochloride (Nektar Therapeutics, Huntsville, Alabama) with acrylic acid chloride and activating the terminal COOH group as *N*-hydroxysuccinimide (NHS) ester (37). Covalent coupling of the glucose derivatives was performed as follows: (i) amino functionalization with aminopropyltriethoxysilane in the gas phase (as described in detail in mal-linker testing and by Riener *et al.* (39) and Ebner *et al.* (38), (ii) reaction of the amino function with the NHS ester function of the cross-linker (39), and (iii) attachment of the ligands to the thiol-reactive groups on the free end of the cross-linker (Fig. 1*C*) (40). In particular, thio-glc (Fig. 1*A*) was coupled to tip-PEG_{5000}-acrylamide (Fig. 1*B*) by incubating these tips in 100 μl of buffer A* (150 mM $NaH_2PO_4 \cdot H_2O$, 1 mM EDTA·Na_2, pH 7.5, adjusted with NaOH) containing 100 mM thio-glc at room temperature for 4 h (19). 20 μl of 100 mM Tris(2-carboxyethyl)phosphine hydrochloride were added into the incubation solution to activate the thiol group of thio-glc. Tips were washed 3 times in buffer A (100 mM NaCl, 50 mM $NaH_2PO_4 \cdot H_2O$, 1 mM EDTA.Na_2, pH 7.5, adjusted with NaOH) and stored in buffer A at 4 °C for at least 3 weeks. For coupling of 2′-aminoethyl β-D-glucopyranoside (hex-glc; Fig. 1*A*) to tip-PEG_{1300}-mal (Fig. 1*B*), 50 μl of AcS-hex-glc (4 mM) in buffer A were mixed with 5 μl of hydroxylamine reagent (500 mM hydroxylamine hydrochloride, 25 mM EDTA, titrated to pH 7.5 with Na_2CO_3) to remove the acetyl group. The AFM tip with the thiol-reactive end group was incubated in this solution for 4 h at room temperature. Tips were washed in buffer A and stored in buffer A at 4 °C for at least 3 weeks. For coupling of hex-phl (Fig. 1*A*) to tip-PEG_{1300}-mal (Fig. 1*B*), the same procedure was used as described for hex-glc.

Cell Culture—RbSGLT1-expressing G6D3 cells, a CHO cell line stably transfected with rabbit SGLT1 generated by Lin *et al.* (41) were grown in 25-cm^2 flasks (BD Falcon™ tissue culture flask, VWR, Vienna, Austria) under 5% CO_2 at 37 °C. This cell line was cultured in Dulbecco's modified Eagle's medium containing high glucose (25 mM) (PAN-Biotech, Aidenberg, Germany) supplemented with 5% fetal calf serum (PAA, Linz, Austria), 1 mM sodium pyruvate (Invitrogen), 2 mM L-glutamine (Invitrogen), minimal essential medium (Invitrogen), and 25 μM β-mercaptoethanol (Invitrogen). Culture medium contained 400 μg/ml sulfate G418 Geneticin (MedPro, Vienna, Austria) to maintain selection of transfected cells. Culture medium was renewed 3 times per week, and the cells were subcultured at 80% confluence. Cell passages below 20 were used

[4] W. Frasch and K. R. H. Kinne, unpublished data.

for all experiments. For AFM investigations, the cells were seeded on 22-mm^2 plastic coverslips from subconfluence to monolayers, and the experiments were performed within 1–5 days after seeding the coverslips.

Cell Viability—At all temperatures, G6D3 cells stably expressing rbSGLT1 (rabbit isoform of SGLT1) appeared to be vital during AFM investigations. Topographical and deflection images of the cells (data not shown), acquired in contact mode using a magnetically driven dynamic force microscope (PicoSPM II, Agilent Technologies, Chandler, AZ) and non-functionalized cantilevers of 0.01–0.03 N/m nominal spring constant, showed a firm attachment on glass slides as the area surrounding the nucleus region revealed to be flat. Typical cells were ~30–70 μm in diameter with a prominent bright zone representing the nucleus with a height of 2–4 μm. The pronounced flatness of the cells and the presence of characteristic morphological features such as the cytoskeleton implied that the cells were alive and vital; this allowed for stable measurements over several hours. Moreover, the cells were very suitable for force spectroscopy measurements due to their elongated spatial dimensions and their low height.

In pilot transport and binding experiments it was found that, as expected, sodium-dependent α-methyl D-glucose uptake at 10 °C was only 5% that of the uptake observed at 37 °C, whereas a slightly increased phlorizin binding was observed.[5]

AFM Force Microscopy/Spectroscopy—All AFM measurements were carried out in Krebs-Ringer-HEPES buffer (120 mM NaCl, 4.7 mM KCl, 2.2 mM $CaCl_2$, 1.2 mM $MgCl_2$, and 10 mM HEPES; the pH was adjusted to 7.4 with Tris-base) using a magnetically driven dynamic force microscope (PicoSPM II, Agilent Technologies, Tempe, AZ). Topographical and deflection images of the cells were acquired in contact mode AFM using non-functionalized cantilevers (Veeco Instruments, Mannheim, Germany) of 0.01–0.03 N/m nominal spring constant in order to record the viability of the cells. For detection of glucose/phlorizin-SGLT1 recognition, force-distance cycles were performed at controlled temperature conditions, *i.e.* 10 °C, 25 °C, and 37 °C, using ligand-functionalized cantilevers (Veeco Instruments) with 0.01–0.03 N/m nominal spring constant in the conventionally contact force spectroscopy mode. In particular, the cells grown on a plastic slide were mounted on an Agilent Peltier-100 sample compartment spanning a temperature range from 0 to 40 °C. A DC power supply device (Mc Voice) was connected with the Peltier-100 to sustain a constant temperature by applying a current. The temperature was controlled by permanently monitoring the resistance of the Peltier element using a digital multimeter (Sky Tronics). A gravity-fed water cooling system was installed to decrease the minimum sample temperature, reduce the power requirement, and prevent overheating of the device when the sample is cooled. The flow rate of the water through the Peltier element was adjusted to 25 ml/min. In addition, the scanner housing was floated with argon gas when the temperature was set to 10 °C to prevent moisture on the glass of the "AFM nose."

Force-distance cycles were recorded with the assistance of a CCD camera for positioning the cantilever above a single cell. At a fixed lateral position an AFM tip carrying a glucose or phlorizin molecule approached (trace) the cell surface and was subsequently retracted (retrace) (see Fig. 2*B*). During this cycle the cantilever deflection (Δz), which can directly be converted into a force (f) according to Hook's law ($f = k\Delta z$, k being the cantilever spring constant), was continuously monitored and plotted *versus* tip-surface separation (*i.e.* distance). Upon approach no bending of the cantilever occurred. As the cantilever touched the surface it deflected upward due to a repulsive tip-sample interaction. Subsequent tip-surface retraction led to relaxation of the cantilever bending until the repulsive force dropped to zero. If a ligand on the tip had bound to a surface protein, an attractive force developed upon retraction, causing the cantilever to bend downward. At a particular unbinding force (f_u) the ligand was detached from the surface-molecule, and the cantilever jumped back to zero deflection.

The interaction efficiency of thio-glc on AA-PEG_{5000}, hex-glc, and hex-phl on maleimide-PEG_{1300}-NHS (mal-PEG_{1300}) was probed at 10 °C, 25 °C, and 37 °C by recording up to 1000 force-distance cycles with a z-range of 1000 N/m/s and a sweep frequency of 1 Hz (amounting to a sweep rate of 2000 nm s^{-1}) on a single cell. Within these 1000 force-distance cycles the position of the cantilever where it touched the cell surface was varied several times. Binding probabilities (the chance for observing an unbinding event within one force-distance cycle) were derived for each linker-molecule-compound at a certain temperature and expressed as the mean value ± S.E. The specificity of the recognition events between SGLT1 and glucose derivatives at each temperature was proven by adding 0.5 mM phlorizin to the buffer solution and thus blocking the substrate interaction sites of SGLT1. The binding probability was acquired for initial conditions (cells in Krebs-Ringer-HEPES buffer without phlorizin), phlorizin-containing conditions, and washout conditions. Binding probabilities are given as the mean values ± S.E.

A close geometrical and chemical fit within the binding pocket has to be accomplished as a prerequisite for molecular recognition; the underlying specific interactions are a distinct class of highly complementary non-covalent bonds composed of several weak interactions such as electrostatic, polar, van der Waals, hydrophobic, and hydrogen bonds. The binding energy E_B, given by the free energy difference between the bound and the free state, is the common parameter to describe the strength of a bond. Ligand-receptor binding is generally a reversible reaction. Thus, the average lifetime of a ligand-receptor bond, $\tau(0)$, is given by the inverse of the kinetic off rate k_{off}. Therefore, ligands will dissociate from receptors without any force applied to the bond at times larger than $\tau(0)$. In contrast, if molecules are pulled faster than $\tau(0)$ the bond will resist and require a force for detachment. The activation energy for the dissociations is the difference in energy between the initial state and the transition state of the highest energy to which the system must be raised before dissociation can occur. In force spectroscopy experiments, the dynamics of pulling on specific receptor-ligand bonds is varied, which leads to detailed structural and kinetic information of the bond breakage. Moreover, energy landscapes of receptor-ligand bonds can be detectable for certain time scales in force-induced unbinding; especially, force

[5] H. Kipp and K. R. H. Kinne, unpublished data.

spectroscopy appears to be a proper tool to discover hidden activation barriers and explore the energy landscape in greater detail.

To study ligand/SGLT1 unbinding forces and kinetic and structural parameters of the binding pocket, the tip approach-and-retract velocities were varied in the range from 1 μm/0.2 s to 1 μm/2 s. Thus, the loading rate, which was determined from the product of the effective spring constant (cantilever spring and bound molecule) times retraction velocity, was varied in the range from $\sim 1.5 \times 10^1$ to $\sim 2 \times 10^4$ pN/s. The measurements were carried out at 10 °C, 25 °C, and 37 °C. Several individual measurements were performed for each linker-molecule compound (thio-glc on AA-PEG_{5000}, hex-glc on to mal-PEG_{1300}, and hex-phl on mal-PEG_{1300}) using cantilevers of 0.01 and 0.02 N/m nominal spring constant. For each tip-ligand system, 1000–2000 force-distance cycles were recorded at each loading rate. Single unbinding events were collected, and the most probable unbinding force (f_u) was plotted against the logarithm of the loading rate (r) to gain the width (x_β) of prominent energy barriers along the dissociation pathway and the dissociation rate constant (k_{off}). In particular, a maximum likelihood approach was employed as a statistical estimation technique to fit a statistical model to the obtained data, thus providing estimations for model's parameters. Here, the consequent unbinding force was plotted against the particular loading rate for every single detected unbinding event. The data points of each recognition event were merged in one dynamic force spectra plot to obtain dynamic aspects of a bond. As an analytical model to estimate for the maximum likelihood of $x_{\beta \text{ and }} k_{off}$, the Evans model was employed. The Bayesian information criterion (BIC) was intended to choose the best model from among several competing/equal models. The BIC was designed to select the best model that describes the data adequately without using too many parameters. The formulation for the BIC is given by,

$$BIC = -2(l(\psi;y) - l(\psi^*;y)) + 2p\log(\sqrt{n}) \qquad \text{(Eq. 1)}$$

where $l(\psi;y)$ is the log-likelihood of the model under consideration, $l(\psi^*;y)$ is the log-likelihood of the most likely model in the subset of models considered, p is the number of parameters fit in the model, and n is the number of observations. Thus, the model with the smallest BIC value is chosen as the best model (41). Student's t test was performed to compare the gained k_{off} and x_β values and account for significant differences.

The spring constant of the cantilevers was determined by using the thermal noise method (42, 43). The deflection sensitivity of the photodetector was determined from the slope of the force-distance plot, taken on the hard bare surface of a glass coverslip. Force-distance cycles were analyzed using Matlab Version 7.1 (MathWorks Inc., Natick, NA) where empirical force distributions of the rupture forces of the unbinding event (probability density function (pdf)) were calculated as described previously (44).

RESULTS

Design of Various Substrate and Inhibitor Derivatives for Tethering to AFM Tips—To investigate SGLT1 interactions at the single-molecule level by AFM, three different compounds were coupled to AFM tips, thio-glc, as an example for the substrate glucose, hex-glc, as representative of alkyl-glucosides, and 3-aminophlorizin (*amino-phl*) (Fig. 1*A*; see "Experimental Procedures"). The molecules were tethered via heterobifunctional PEG linkers varying in length (N) and end-group (TRG) having the general structure TRG-PEG_N-NHS (see Fig. 1, *B* and *C*), "TRG" denoting a thiol-reactive group (maleimide or acrylamide) and "NHS" indicating a reactive NHS ester. In detail, thioglucose was linked to the tip via a long (~30–40 nm) acrylamide-PEG-linker (AA-PEG_{5000}) using a well established three-step protocol (see Fig. 1*C*). The latter has one of the thinnest and least bulky functional PEG-chain end groups. Amino ethyl β-D-glucopyranoside as well as 3-aminophlorizin was coupled to the tip using a short (~8 nm) mal-PEG_{1300}.

Single Molecule Recognition of SGLT1—A scheme of single-molecule recognition force detection of a glucose derivative-SGLT1 complex on living G6D3 cells by using AFM is illustrated in Fig. 2*A*. In this so-called force-distance mode, the deflection angle of the cantilever is measured as a function of the vertical position of the cantilever. A typical force curve (retraction) for a single molecule glucose-SGLT1 binding event on the surface of a G6D3 cell with a ligand-conjugated tip is shown in Fig. 2*B*. The specificity of the interaction between all tip-tethered glucose derivatives and SGLT1 on the cell membrane could be confirmed by masking the substrate binding site of SGLT1 with free phlorizin (see the *inset* in Fig. 2*B* and Fig. 3). The number of recognition events dropped significantly, to ~20% of the unblocked conditions. The same low binding probability was observed when parental CHO cells not expressing SGLT1 were investigated (data not shown).

Binding Behavior of Thioglucose, Alkyl-glucose, and Aminophlorizin Tethered AFM Cantilevers at Different Temperatures—It was found that SGLT1 could specifically be detected at 10 °C, 25 °C, and 37 °C when living cells were probed using cantilevers carrying the substrate or inhibitors. The observed binding probabilities (probability of finding an unbinding event in force-distance cycles) of all tips to SGLT1 from several experiments ranged from 9 to 27% but were not statistically different.

Comparing the binding probability of thioglucose on AA-PEG_{5000} at different temperatures, the binding probability was low at 10 °C (8.7 ± 2.28%) and increased significantly for 25 °C (14.62 ± 3.69%) and further at 37 °C (26.72 ± 4.56%) (Fig. 4*A*). It is noteworthy that at 37 °C thioglucose on AA-PEG_{5000} shows the highest binding probabilities of all derivatives tested. The interaction of hexyl-glucose on mal-PEG_{1300} with the cells was not altered significantly by changing the temperature, as the binding probability ranged from 11.3 ± 1.16 to 15.6 ± 2.03% for all temperatures (Fig. 4*B*). Similarly, the recognition events for aminophlorizin on mal-PEG_{1300} showed only small changes: a slightly increased binding at 37 °C (19.38 ± 3.2%) compared with 10 °C (16.9 ± 1.55%) and lesser binding probability at 25 °C (11.13 ± 1.00%) (Fig. 4*C*).

Kinetic and Structural Parameters of the Binding Pockets—Experiments were performed at various tip-retraction velocities, leading to a force spectrum in dependence on the loading rate (pulling velocity times effective spring constant). Unbinding forces for thioglucose on AA-PEG_{5000}, hexyl-glucose on

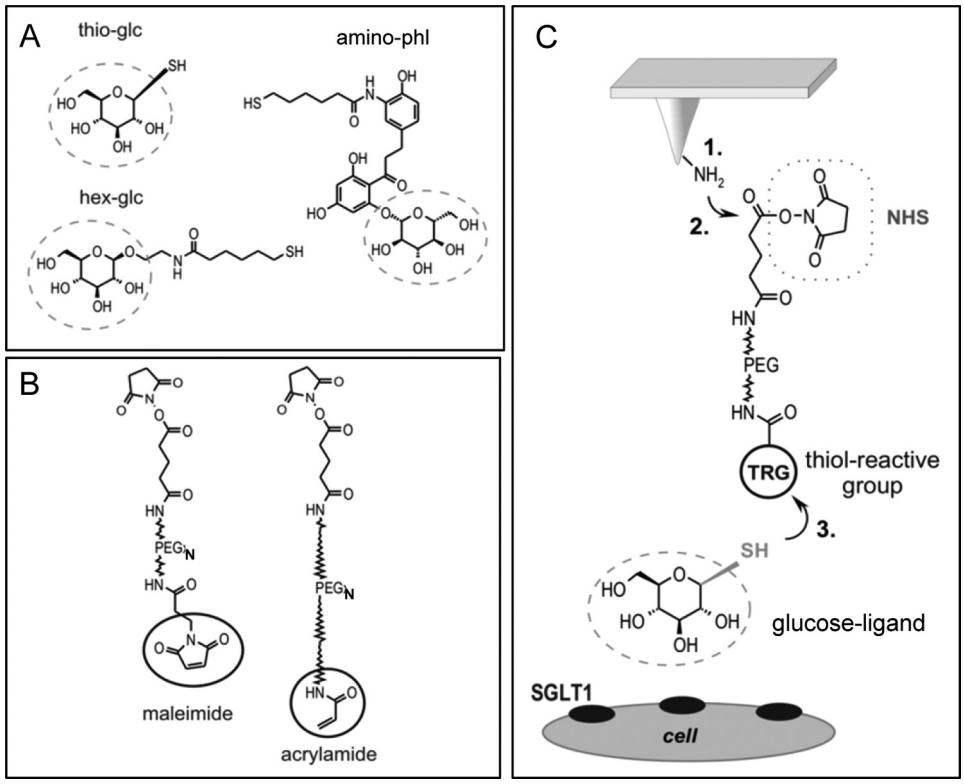

FIGURE 1. **Linkage of substrates and inhibitors of SGLT1to the AFM tip via heterobifunctional PEG linker by a three-step protocol.** Thio-glc, hex-glc, and AcS-aminophlorizin (*amino-phl*) (*A*) were coupled to cross-linkers varying in lengths having a maleimide end group (~8 nm) or an acrylamide-end group (~30–40 nm) (*B*). *C*, amino groups were generated on the silicon nitride AFM cantilever tip using aminopropyltriethoxysilane (*step 1*) to attach the flexible distensible PEG-linker covalently via its NHS end to the tip (*step 2*). The ligand was linked to the free thio-reactive end of the PEG chain (*step 3*). Thioglucose was coupled to the acrylamide-linker, hexyl-glucose, and aminophlorizin were bound to the maleimide-linker. Circles in *B* and *C* indicate the thio-reactive group (*TRG*). In *C* the *dotted line* circles the ligand, which is coupled to the PEG linker.

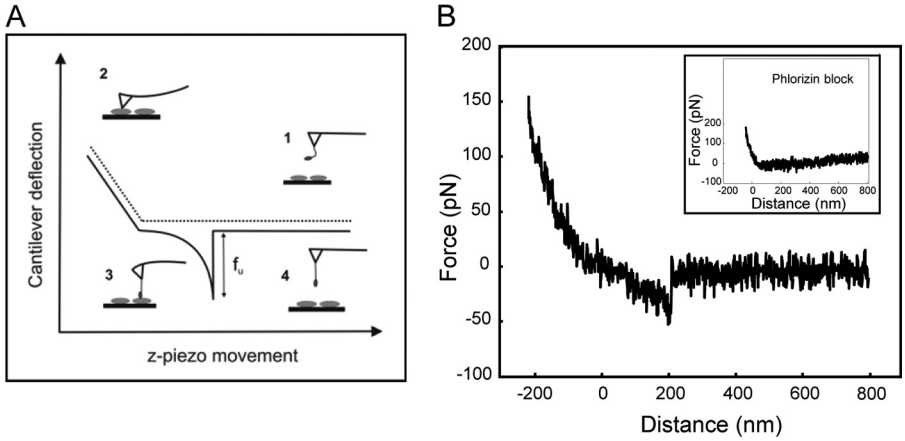

FIGURE 2. **Single molecule recognition of SGLT1 on the surface of living cells.** *A*, schematic representation of a force-distance cycle, where the cantilever approached the cell surface and subsequently retracted (*solid line*). The deflection angle of the cantilever remained zero (*1*) until the tip contacted the sample surface from where the cantilever was bent upward (*2*). Upon retraction a force signal with a distinct shape occurred when an interaction between the ligand and a receptor occurred (*3*). The cantilever was increasingly bent downward until the bond broke at a defined unbinding force f_u required to break a single ligand-receptor interaction (*4*). *B*, force curves show specific interactions between thioglucose coupled via an acrylamide-linker and SGLT1 upon tip-surface retraction. The specific recognition disappeared in the presence of phlorizin (*inset*).

mal-PEG_{1300}, and aminophlorizin on mal-PEG_{1300} were determined for retraction speeds in the range between 1.5×10^1 to $\sim 2 \times 10^4$ pN/s. All collected force-distance cycles were evaluated by selecting every single unbinding event and generating the probability density function of the force, effective spring constant, and length. The individual forces of each unbinding event were plotted against the logarithm of the loading rate and thus merged into one particular force spectrum (45). The results obtained for thioglucose on AA-PEG_{5000} probed at different temperatures are shown in Fig. 5. As expected (46, 47), the forces increased with increasing loading rates. Subsequently, data were analyzed using a maximum likelihood approach yielding a comprehensible estimation for the width of the energy barrier, x_β, and the dissociation rate constant, k_{off}. Herein, a cloud of data points was gained to which a maximum likelihood fit using the Evans model as the analytical model was

applied to estimate x_β and k_{off} (Fig. 5; also see "Experimental Procedures"). From these, x_β and k_{off} of the SGLT1·thioglucose bond were calculated. As illustrated in Fig. 5, for instance, the width of the energy barrier, x_β, and dissociation rate constant, k_{off}, at 37 °C were 6.24 ± 0.08 Å and 0.26 ± 0.02 s^{-1}, respectively (Fig. 5*C*).

The obtained forces and the corresponding loading rates of all investigated cantilevers at a distinct temperature, *i.e.* 10 °C, 25 °C, or 37 °C, were merged into one dynamic force spectra plot (Fig. 6). Thus, hundreds of particular unbinding events were taken into account individually making estimates for the structural and kinetic parameter more precise. The values obtained for dissociation rate and the width of the energy barriers are listed in Table 1. Thioglucose on AA-PEG_{5000} revealed the lowest dissociation rate constant, k_{off} (0.26 ± 0.02 s^{-1}), at 37 °C indicating that the lifetime of the SGLT1·thioglucose complex is longest at this temperature compared with 25 °C (0.83 ± 0.07 s^{-1}) and 10 °C (0.6 ± 0.05 s^{-1}). These values were significantly different, with $p < 0.001$. In contrast, hexyl-glucose bound to mal-PEG_{1300} dissociated from the transporter in a quite similar time scale at each temperature (k_{off} = 0.41 ± 0.03 s^{-1} at 10 °C, 0.50 ± 0.07 s^{-1} at 25 °C and 0.4 ± 0.07 s^{-1} at 37 °C). However, aminophlorizin on mal-PEG_{1300} showed an inversed dissociation behavior compared with thioglucose, as the lifetime of the aminophlorizin·SGLT1 complex is shortened with increasing temperatures. Thus, aminophlorizin was the molecule that dissociated significantly faster at 37 °C (k_{off} = 1.00 ± 0.06 s^{-1}) than at 10 °C (k_{off} = 0.34 ± 0.03 s^{-1}).

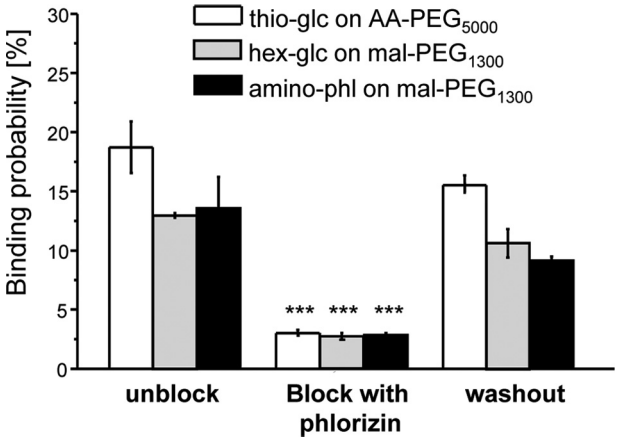

FIGURE 3. **Specific interaction of glucose and inhibitors at 37 °C.** Data of one typical experiment are presented for each cantilever, probed in different conditions: initial condition (*first column*), block condition (*second column*), and washout condition (*third column*). Values are the mean ± S.E. for n = 2000–3000, where 2–3 different cells were probed at each condition. The specificity of the recognition events could be demonstrated by a significantly reduced binding probability in the presence of phlorizin when compared with control levels (initial condition) with $p < 0.005$. After a careful washout procedure the interaction increased again. *amino-phl*: 3-aminophlorizin.

Moreover, the single molecular binding energy width for glucose/inhibitor/cotransporter interactions could be extracted from the plot of unbinding force *versus* the loading rate (see "Experimental Procedures"). The width of the energy barrier, x_β, can thereby be taken as a measure for the location of the maximum energy barrier within the binding pocket. The obtained values for the x_β of thioglucose on AA-PEG_{5000} increased with increasing temperatures (x_β = 3.96 ± 0.08 Å at 10 °C, 4.99 ± 0.1 Å at 25 °C, and 6.24 ± 0.08 Å at 37 °C). x_β for thioglucose on AA-PEG_{5000} at 37 °C was largest among all linker compounds investigated. The length scales of the binding pocket for hexyl-glucose on mal-PEG_{1300} probed at different temperatures were also altered within a p value < 0.01, showing the highest value at 10 °C (x_β = 3.48 ± 0.05 Å) and the lowest at 37 °C (x_β = 2.75 ± 0.1 Å). Similar values for x_β were observed for aminophlorizin on mal-PEG_{1300} at 10 °C (x_β = 3.23 ± 0.06 Å) and 37 °C (x_β = 2.93 ± 0.04 Å).

DISCUSSION

In the present study SGLT1 was mapped on the membrane of living G6D3 cells stably expressing the transporter by AFM cantilevers being loaded with 1-thio-β-D-glucose, modified amino-hexyl-glucose, and aminophlorizin. The binding behavior, *e.g.* binding probability, interaction forces, etc. of particular ligands was ascertained at different temperatures by performing single molecule recognition force spectroscopy experiments. Moreover, new structural and kinetic parameters of the

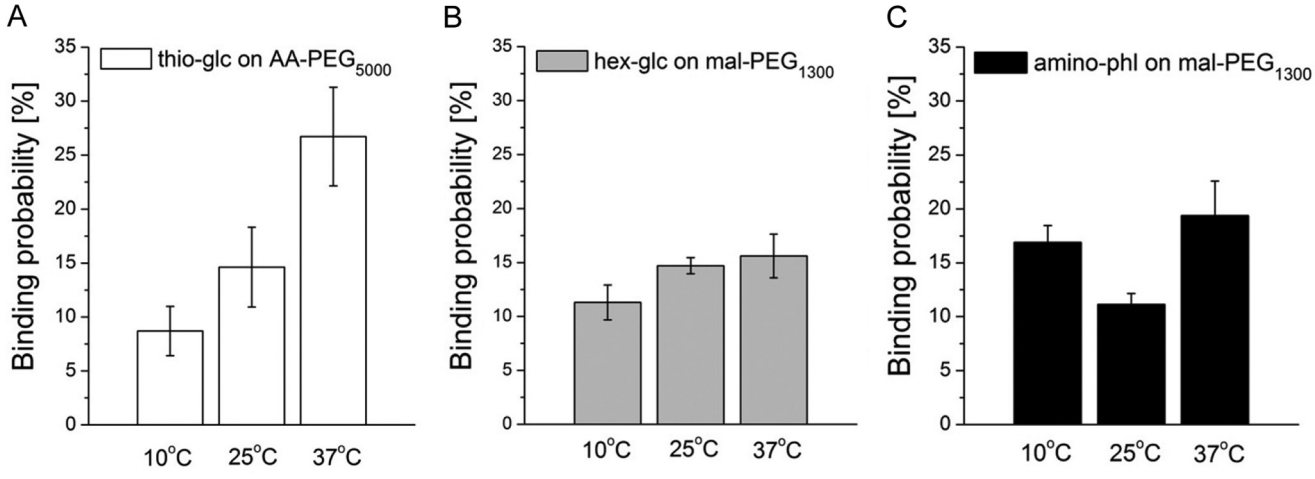

FIGURE 4. **Binding probabilities of glucose, hexyl-glucose, and aminophlorizin at different temperatures.** The interaction between thioglucose on AA-PEG_{5000} (*A*), hexyl-glucose on mal-PEG_{1300} (*B*), and aminophlorizin (*C*) on mal-PEG_{1300} was studied at 10 °C, 25 °C, and 37 °C using the same cantilever and the same cells. Values are the mean ± S.E. of three to five different cantilevers and two different cells for one cantilever. On each cell up to 1000 force-distance cycles were recorded.

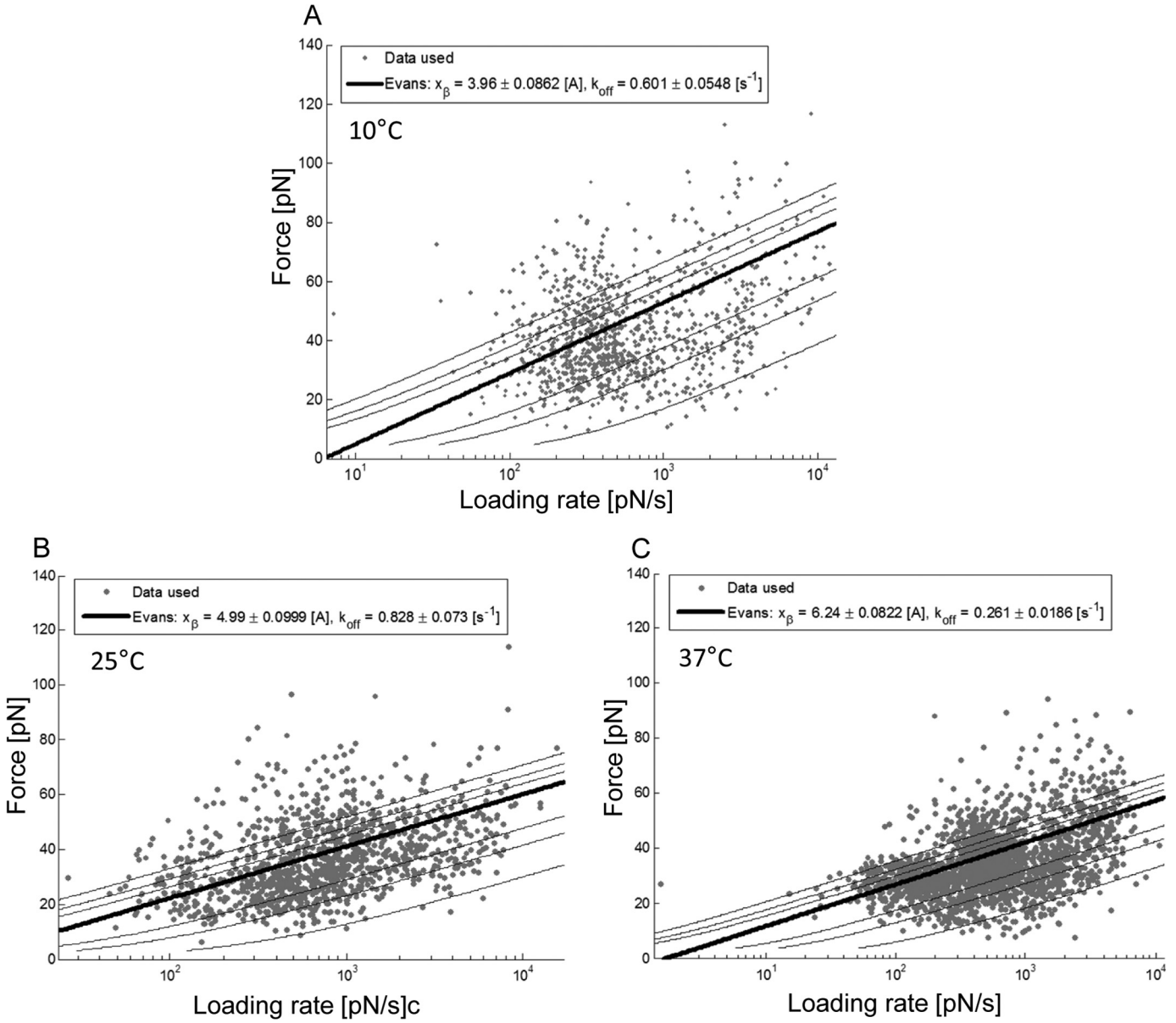

FIGURE 5. **Dynamic force spectroscopy spectra of thioglucose on AA-PEG_{5000} probed at different temperatures.** Glucose/SGLT1 recognition was investigated at different tip-retraction velocities to gain dynamic aspects of bond rupture in various temperatures, *i.e.* 10 °C (*A*), 25 °C (*B*), and 37 °C (*C*). By applying a maximum likelihood approach the most likely and accurate values for the length scale x_β and the kinetic off rate k_{off} were estimated. *A*, at 10 °C x_β of thioglucose on AA-PEG_{5000} was lowest, and the sugar dissociated fastest. *B*, at 25 °C x_β as well as k_{off} were increased. *C*, notably, at 37 °C x_β was even further increased, whereas the dissociation was slower than at 10 °C. Data were obtained from merging results from six different cantilevers.

interactions of SGLT1 with glucose and transport inhibitors could be gained.

New SGLT1 Sensors—In the current study new coupling chemistry for tethering thioglucose, hexyl-glucose, and aminophlorizin to the AFM tip was developed. Previously, AFM studies on SGLT1 had been performed mainly with a vinylsulfone linker between the PEG chain and thioglucose or a modified 3′ aminophlorizin (19, 20, 48). By using acrylamide as the thioreactive group to attach thioglucose to PEG_{5000}, the size (and charge) of the thioester linkage is reduced compared with vinylsulfone-PEG_{800}. In addition, the PEG chain is extended, providing the least bulky and most flexible sugar probe used until now (Fig. 1*B*).

In AcS-hexyl-glucose, terminally coupled to the thioreactive group of the PEG chain, a long stretch of an alkyl chain is exposed, allowing additional interactions of this entity with the transporter similar to those occurring with free hexyl-glucose (26). In addition, phlorizin was tethered to the AFM tip via a C6 chain to an amino group at the C3 atom of its aromatic ring B; this provides more mobility to phlorizin on the cantilever tip but leaves the major binding sites of its aglucon moiety, the 4′-OH and 6′-OH of the adjacent aromatic ring A, freely accessible to SGLT1 (49). Replacement of vinylsulfone by maleimide accelerates the coupling reaction.

With all three newly synthesized sensors a specific recognition of SGLT1 can occur, as the major binding sites of glucose are freely accessible. Thus, a proper fitting of the sugar moieties into the binding pocket of SGLT1, mainly formed by transmembrane helices 10–13, can be achieved (20, 50–53). The specificity of interaction of the probes was demonstrated first of

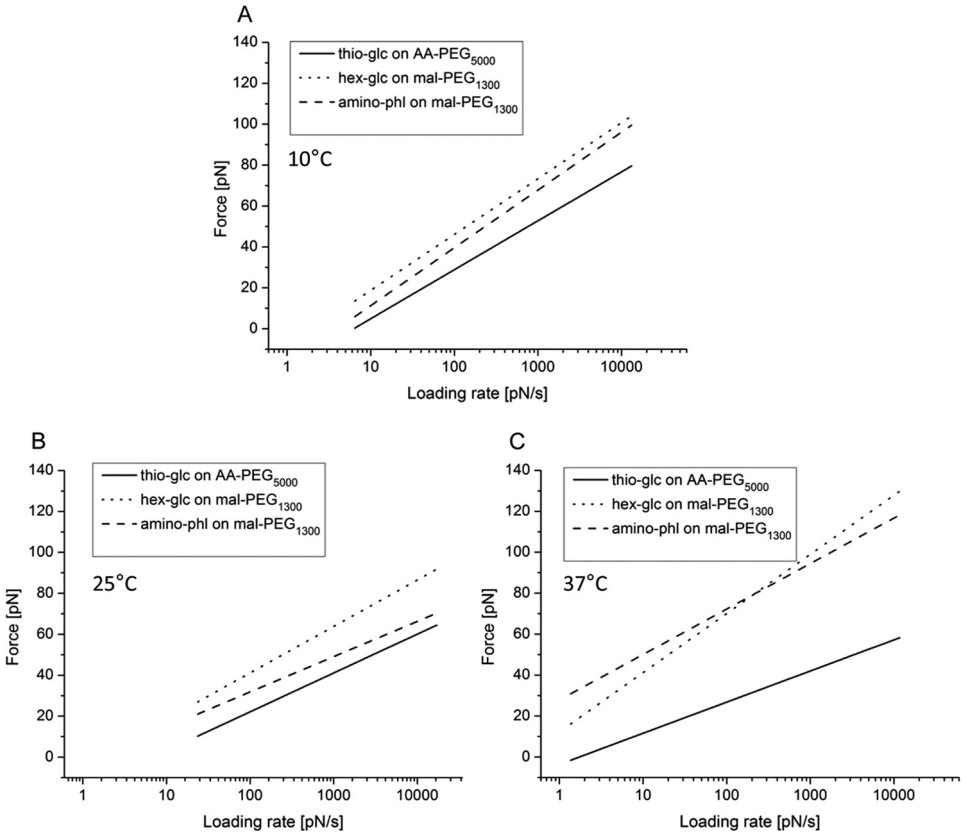

FIGURE 6. **Dynamic force spectra of the different SGLT1 ligand complexes at different loading rates.** The most probable unbinding forces were plotted against the logarithm of the loading rate. Comparisons of force spectra with thioglucose on AA-PEG_{5000}, hexyl-glucose on mal-PEG_{1300}, and aminophlorizin on mal-PEG_{1300} at 10 °C (*A*), 25 °C (*B*) , and 37 °C (*C*) are shown.

TABLE 1

Kinetic property of glucose, hexyl-glucose, and aminophlorizin binding to rbSGLT1

The values were obtained from the experiments depicted in Fig. 6. k_{off} of thioglucose on AA-PEG_{5000} at 37 °C compared with k_{off} of thioglucose on AA-PEG_{5000} at 10 °C and 25 °C and k_{off} of aminophlorizin on mal-PEG_{1300} at 37 °C when compared with k_{off} of aminophlorizin on mal-PEG_{1300} at 10 °C and 25 °C were significantly different. $x_{ß}$ of thioglucose on AA-PEG_{5000} at 37 °C when compared with $x_{ß}$ of the other ligands was significantly different.

	Width of the energy barrier, $x_{ß}$			Dissociation rate constant, k_{off}		
SGLT1 sensors	10 °C	25 °C	37 °C	10 °C	25 °C	37 °C
		Å			s^{-1}	
Thio-glc on AA-PEG_{5000}	3.96 ± 0.08	4.99 ± 0.1	6.24 ± 0.08[a]	0.60 ± 0.05	0.83 ± 0.07	0.26 ± 0.02[b]
hex-glc on mal-PEG_{1300}	3.48 ± 0.05	3.18 ± 0.1	2.75 ± 0.1	0.41 ± 0.03	0.50 ± 0.07	0.40 ± 0.07
Amino-phl on mal-PEG_{1300}	3.23 ± 0.06	4.28 ± 0.1	2.93 ± 0.04	0.34 ± 0.03	0.54 ± 0.07	1.00 ± 0.06[b]

[a] $p < 0.005$.
[b] $p < 0.001$.

all by the fact that a significant number of unbinding events was only observed in CHO cells transfected with the *sglt1* gene. In addition, for all probes the number of unbinding events was almost identical, and low concentrations of phlorizin reversibly reduced the binding.

Effect of Temperature on SGLT1 Properties—In the current study SGLT1 was investigated in living cells incorporated into the plasma membrane. Temperature changes can affect such a system in various ways. With regard to the membrane, phospholipids undergo phase transitions and change their fluidity. Previous studies have shown that SGLT1 activity changes in parallel to the changes in fluidity when it is incorporated into liposomes composed of phospholipids with different transition points (54). This strong dependence is probably due to the fact that ~40% of the Trps responsible for hSGLT1 fluorescence are in close contact to the membrane phospholipids (23).

The SGLT1 protein is postulated to undergo a series of conformational changes while transporting glucose from the extracellular side of the cell membrane into the cytoplasm in an alternating accessibility model. Starting with an outward-facing configuration, sodium binding opens up access to the sugar translocation pathway. Thereafter, glucose is bound and occluded in the translocation site. This is followed by a conformational change from an outward-facing occluded state to an inward-facing occluded state. Upon opening of the inward gate, the Na^+ ions and sugar are released into the cell interior. The transport cycle is completed by the transition from the inward-facing ligand-free state to the outward-facing ligand-free state (15). This transport cycle involves rearrangement of intramolecular binding sites as well as changes in the orientation of transmembrane helices. By changing the temperature, the conformational equilibrium to the various states might be altered.

Thermal fluctuations of proteins are in general important for biological activity (55); thus the temperature changes in this work may modulate the protein flexibility, and folding and orientation of substructures within the membrane can be affected or accessibility to the sugar binding residues. Finally the interaction forces between ligands and proteins (hydrogen bonding and Coulomb and van der Waal forces) are temperature-dependent (56).

At 10 °C, which is below the transition point of the membrane lipids, SGLT1 is probably constrained in its structural movements and trapped in non-transporting conformational states. Interestingly, even at this temperature, SGLT1 was able to interact specifically with all ligands, suggesting that sodium and sugars can be bound by the transporter. Evidence for this interaction can also be derived from phlorizin binding studies where a sodium-dependent, glucose inhibitable binding was found.[4,5] This implies that the opening of the vestibule and the initial hydrophilic sugar binding cavity is rather temperature-independent as it occurs at the surface of the transporter. Similar conclusions can be drawn from tryptophan fluorescence studies with purified hSGLT1 (57). With an increase of the temperature to 25 °C, all binding probabilities increase similar to the transport activity and turnover rate; at a higher turnover rate probably more SGLT1s in the outward open conformation face the membrane surface per time unit; thus, more binding events can occur. At 37 °C, another increase in binding probability is observed for thioglucose on AA-PEG_{5000} but not for hexyl-glucose or aminophlorizin on mal-PEG_{1300}. This result might suggest that at this temperature the thioglucose probe recognized SGLT1 in more than one conformation. Further evidence for this assumption is presented below.

Dynamic force spectroscopy measurements track the dynamic behavior of SGLT1 upon substrate and inhibitor binding. Here, structural and kinetic parameters of their SGLT1 bond were gained by varying the cantilever retraction speed over several orders of magnitude. In particular, when probed at 10 °C, thioglucose was detached faster from SGTL1 than at 25 °C and 37 °C. Thermodynamically, the opposite would be expected for simple binding reactions. The long-lasting average lifetime of the SGLT1·thioglucose-AA-PEG_{5000} bond at 37 °C might be explained by additional conformation of SGLT1 in which thioglucose on the long AA-PEG_{5000}-linker is able to penetrate deeper into the translocation pathway of the transporter, beyond the initial sugar binding site. The very slim reactive end group of the PEG linker could facilitate this entry. This assumption is supported by the previously reported increased unbinding force when thioglucose is coupled to the AFM tip via an acrylamide linker as compared with the bulkier vinylsulfone linker (58). The highest value for the width of the binding pocket observed for thioglucose on AA-PEG_{5000} at 37 °C (see Table 1) provides further evidence. The latter can be directly related to the number of protein residues contributing to binding sites (40). Hirayama *et al.* (60), 2007) reported that 3 residues between transmembrane helices 10 and 13 play a direct role in sugar binding and translocation from the external environment, 3 more face the binding site, and 8 further residues, although not contributing to the binding of sugar directly, affect sugar recognition. Thus, it might be assumed that at 37 °C some of the primarily not accessible binding sites further down in the translocation pathway are reached by thioglucose on AA-PEG_{5000} (21). A sequential multistep mechanism for sugar recognition and translocation has also been proposed based on prior AFM investigations (20).

Thioglucose on AA-PEG_{5000} and aminophlorizin on mal-PEG_{1300} showed an inverse behavior in k_{off} when compared at 10 °C and 37 °C, and thioglucose on AA-PEG_{5000} was bound longest to the transporter at 37 °C among all probed derivatives and temperatures, whereas aminophlorizin yielded the highest dissociation rate constant (shortest time) at 37 °C. The findings for phlorizin dissociation are in good agreement with previous studies (3) as inhibitor association and dissociation were reported to be enhanced at 37 °C (59–61). This observation suggests that the glucose moiety of phlorizin is not capable of penetrating as deep into the translocation pathway as thioglucose on AA-PEG_{5000} due to steric hindrance by the aromatic aglucon. This assumption is supported by the lower width of the energy barrier. PEG is an ideal force transducer (62), and the force spectrum measured with dynamic force spectroscopy is largely independent on length of the handle (45, 63) through which the ligands are attached to the AFM tips. It thus seems improbable that the observed effects are due to the difference in length of the linker PEG chains of the two probes, ~170 Å for phlorizin and ~700 Å for thioglucose. Moreover, the hydrophilic cavity of the transporter, which leads to the translocation, is only 7 Å deep (57).

One has to postulate, in addition, that the aglucon binding site of SGLT1 on the membrane surface is altered at this temperature. Previous studies by our groups have shown that, in rbSGLT1, loops 13–14 facing the extracellular space is critically involved in the binding of the aglucon (64). *In vitro* studies suggest that the loop has a substructure of two small helices and interacts in several regions with membrane phospholipids (10, 65). These structural requirements for a tight interaction with the aglucon might be partly lost due to the increased lipid fluidity, and thereby overall binding affinity is reduced.

Hexyl-glucose, as a model for the interaction between SGLT1 and alkyl-glucosides, shows binding probabilities quite similar to those obtained for the aminophlorizin-tagged probe; with regard to k_{off} and width of the energy barrier it lies in between thioglucose on AA-PEG_{5000} and aminophlorizin. Thus, as expected, the sugar moiety and the alkyl chain are involved in the binding to SGLT1; however, the relative role of the aglucon-receptor interactions seems to be less important for the overall binding reaction. This is also reflected in the 10× lower affinity to the carrier in transport studies (26).

In conclusion, a binding schematic for the substrate and transport inhibitors at different temperatures might be hypothesized; (i) glucose, phlorizin, and hexyl-glucose at all temperatures interact with SGLT1, the latter two via both sugar and aglucon binding sites located on the membrane surface, (ii) with increasing temperature the sugar translocation pathway opens, and additional binding sites for glucose become available and accessible, and (iii) the increase in temperature perturbs the conformation of the aglucon binding sites required for optimum interaction with transport inhibitors. The distinct temperature dependence observed in the current study sup-

ports the existence of multiple steps in the outward-facing translocation pathway of SGLT1, from the initial sugar binding followed by stereo-selection to occlusion of the sugar. It also corroborates the assumption of a two-site two-step mechanism for the binding of transport inhibitors. To describe the dynamical behavior of SGLT1 upon substrate and inhibitor binding more precisely, *e.g.* determining distinct binding sites or account for distinct conformations, single-molecule force spectroscopy experiments combined with mutagenesis studies would be required in which specific residues involved in sugar binding and translocation are exchanged. Furthermore, it has to be determined whether the changes induced by the different temperatures reflect conformations occurring in the normal translocation cycle.

Finally, these studies demonstrate that AFM force spectroscopy is a useful method for exploring the functional dynamics of membrane transporters and paves the way for investigating the influence of transport-inhibiting substances potentially applicable as therapeutics on the single molecule level under near-native conditions.

REFERENCES

1. Crane, R. K. (1977) The gradient hypothesis and other models of carrier-mediated active transport. *Rev. Physiol. Biochem. Pharmacol.* **78,** 99–159
2. Wright, E. M., Loo, D. D., and Hirayama, B. A. (2011) Biology of human sodium glucose transporters. *Physiol. Rev.* **91,** 733–794
3. Hummel, C. S., Lu, C., Loo, D. D., Hirayama, B. A., Voss, A. A., and Wright, E. M. (2011) Glucose transport by human renal Na^+/D-glucose cotransporters SGLT1 and SGLT2. *Am. J. Physiol. Cell Physiol.* **300,** C14–C21
4. Wright, E. M. (1998) I. Glucose galactose malabsorption. *Am. J. Physiol.* **275,** G879–G882
5. Castaneda, F., Burse, A., Boland, W., and Kinne, R. K. (2007) Thioglycosides as inhibitors of hSGLT1 and hSGLT2: potential therapeutic agents for the control of hyperglycemia in diabetes. *Int. J. Med. Sci.* **4,** 131–139
6. Kinne, R. K., and Castaneda, F. (2011) SGLT inhibitors as new therapeutic tools in the treatment of diabetes. *Handb. Exp. Pharmacol.* **203,** 105–126
7. Castaneda, F., and Kinne, R. K. (2005) A 96-well automated method to study inhibitors of human sodium-dependent D-glucose transport. *Mol. Cell Biochem.* **280,** 91–98
8. Hirayama, B. A., Díez-Sampedro, A., and Wright, E. M. (2001) Common mechanisms of inhibition for the Na^+/glucose (hSGLT1) and Na^+/Cl^-/GABA (hGAT1) cotransporters. *Br. J. Pharmacol.* **134,** 484–495
9. Tyagi, N. K., Kumar, A., Goyal, P., Pandey, D., Siess, W., and Kinne, R. K. (2007) D-Glucose recognition and phlorizin-binding sites in human sodium/D-glucose cotransporter 1 (hSGLT1): a tryptophan scanning study. *Biochemistry* **46,** 13616–13628
10. Raja, M. M., Tyagi, N. K., and Kinne, R. K. (2003) Phlorizin recognition in a C-terminal fragment of SGLT1 studied by tryptophan scanning and affinity labeling. *J. Biol. Chem.* **278,** 49154–49163
11. Wright, E. M., Hirayama, B. A., and Loo, D. F. (2007) Active sugar transport in health and disease. *J. Intern. Med.* **261,** 32–43
12. Lin, J., Kormanec, J., Homerová, D., and Kinne, R. K. (1999) Probing transmembrane topology of the high-affinity sodium/glucose cotransporter (SGLT1) with histidine-tagged mutants. *J. Membr. Biol.* **170,** 243–252
13. Watanabe, A., Choe, S., Chaptal, V., Rosenberg, J. M., Wright, E. M., Grabe, M., and Abramson, J. (2010) The mechanism of sodium and substrate release from the binding pocket of vSGLT. *Nature* **468,** 988–991
14. Wimmer, B., Raja, M., Hinterdorfer, P., Gruber, H. J., and Kinne, R. K. (2009) C-terminal loop 13 of Na^+/glucose cotransporter 1 contains both stereospecific and non-stereospecific sugar interaction sites. *J. Biol. Chem.* **284,** 983–991
15. Sala-Rabanal, M., Hirayama, B. A., Loo, D. D., Chaptal, V., Abramson, J., and Wright, E. M. (2012) Bridging the gap between structure and kinetics of human SGLT1. *Am. J. Physiol. Cell Physiol.* **302,** C1293–C1305
16. Hinterdorfer, P., Baumgartner, W., Gruber, H. J., Schilcher, K., and Schindler, H. (1996) Detection and localization of individual antibody-antigen recognition events by atomic force microscopy. *Proc. Natl. Acad. Sci. U.S.A.* **93,** 3477–3481
17. Hinterdorfer, P., and Dufrêne, Y. F. (2006) Detection and localization of single molecular recognition events using atomic force microscopy. *Nat. Methods* **3,** 347–355
18. Wildling, L., Rankl, C., Haselgrübler, T., Gruber, H. J., Holy, M., Newman, A. H., Zou, M. F., Zhu, R., Freissmuth, M., Sitte, H. H., and Hinterdorfer, P. (2012) Probing binding pocket of serotonin transporter by single molecular force spectroscopy on living cells. *J. Biol. Chem.* **287,** 105–113
19. Puntheeranurak, T., Wildling, L., Gruber, H. J., Kinne, R. K., and Hinterdorfer, P. (2006) Ligands on the string: single-molecule AFM studies on the interaction of antibodies and substrates with the Na^+-glucose cotransporter SGLT1 in living cells. *J. Cell Sci.* **119,** 2960–2967
20. Puntheeranurak, T., Wimmer, B., Castaneda, F., Gruber, H. J., Hinterdorfer, P., and Kinne, R. K. (2007) Substrate specificity of sugar transport by rabbit SGLT1: single-molecule atomic force microscopy versus transport studies. *Biochemistry* **46,** 2797–2804
21. Puntheeranurak, T., Kasch, M., Xia, X., Hinterdorfer, P., and Kinne, R. K. (2007) Three surface subdomains form the vestibule of the Na^+/glucose cotransporter SGLT1. *J. Biol. Chem.* **282,** 25222–25230
22. Diedrich, D. F. (1966) Competitive inhibition of intestinal glucose transport by phlorizin analogs. *Arch. Biochem. Biophys.* **117,** 248–256
23. Kumar, A., Tyagi, N. K., and Kinne, R. K. (2007) Ligand-mediated conformational changes and positioning of tryptophans in reconstituted human sodium/D-glucose cotransporter1 (hSGLT1) probed by tryptophan fluorescence. *Biophys. Chem.* **127,** 69–77
24. Loo, D. D., Hirayama, B. A., Cha, A., Bezanilla, F., and Wright, E. M. (2005) Perturbation analysis of the voltage-sensitive conformational changes of the Na^+/glucose cotransporter. *J. Gen. Physiol.* **125,** 13–36
25. Oulianova, N., Falk, S., and Berteloot, A. (2001) Two-step mechanism of phlorizin binding to the SGLT1 protein in the kidney. *J. Membr. Biol.* **179,** 223–242
26. Kipp, H., Lin, J. T., and Kinne, R. K. (1996) Interactions of alkylglucosides with the renal sodium/D-glucose cotransporter. *Biochim. Biophys. Acta* **1282,** 125–130
27. Raja, M. M., Kipp, H., and Kinne, R. K. (2004) C-terminus loop 13 of Na^+ glucose cotransporter SGLT1 contains a binding site for alkyl glucosides. *Biochemistry* **43,** 10944–10951
28. Lee, G. U., Chrisey, L. A., and Colton, R. J. (1994) Direct measurement of the forces between complementary strands of DNA. *Science* **266,** 771–773
29. Florin, E. L., Moy, V. T., and Gaub, H. E. (1994) Adhesion forces between individual ligand-receptor pairs. *Science* **264,** 415–417
30. Rico, F., and Moy, V. T. (2007) Energy landscape roughness of the streptavidin–biotin interaction. *J. Mol. Recognit.* **20,** 495–501
31. De Smedt, H., and Kinne, R. (1981) Temperature dependence of solute transport and enzyme activities in hog renal brush border membrane vesicles. *Biochim. Biophys. Acta* **648,** 247–253
32. Ni, J., Singh, S., and Wang, L. X. (2003) Synthesis of maleimide-activated carbohydrates as chemoselective tags for site-specific glycosylation of peptides and proteins. *Bioconjug. Chem.* **14,** 232–238
33. Wruss, J., Pollheimer, P. D., Meindl, I., Reichel, A., Schulze, K., Schöfberger, W., Piehler, J., Tampé, R., Blaas, D., and Gruber, H. J. (2009) Conformation of receptor adopted upon interaction with virus revealed by site-specific fluorescence quenchers and FRET Analysis. *J. Am. Chem. Soc.* **131,** 5478–5482
34. Kamruzzahan, A. S., Ebner, A., Wildling, L., Kienberger, F., Riener, C. K., Hahn, C. D., Pollheimer, P. D., Winklehner, P., Hölzl, M., Lackner, B., Schörkl, D. M., Hinterdorfer, P., and Gruber, H. J. (2006) Antibody linking to atomic force microscope tips via disulfide bond formation. *Bioconjug. Chem.* **17,** 1473–1481
35. Lin, J. T., Hahn, K. D., and Kinne, R. (1982) Synthesis of phlorizin derivatives and their inhibitory effect on the renal sodium/D-glucose cotransport system. *Biochim. Biophys. Acta* **693,** 379–388
36. Wildling, L. (2008) *Biofunktionalisierung von Atomkraftmikroskopiespitzen mit einem breit anwendbaren, modularen Linkersystem.* Ph.D. thesis. The Johannes Kepler University, Linz, Austria

37. Wildling, L. (2005) *Biofunktionalisierung von Messspitzen für die Rastersondenmikroskopie.* Diploma thesis. The Johannes Kepler University, Linz, Austria
38. Ebner, A., Hinterdorfer, P., and Gruber, H. J. (2007) Comparison of different aminofunctionalization strategies for attachment of single antibodies to AFM cantilevers. *Ultramicroscopy* **107,** 922–927
39. Riener, C. K., Stroh, C. M., Ebner, A., Klampfl, C., Hall, A. A., Romanin, C., Lyubchenko, Y. L., Hinterdorfer, P., and Gruber, H. J. (2003) Simple test system for single molecule recognition force microscopy. *Anal. Chim. Acta* **479,** 59–75
40. Strunz, T., Oroszlan, K., Schäfer, R., and Güntherodt, H. J. (1999) Dynamic force spectroscopy of single DNA molecules. *Proc. Natl. Acad. Sci. U.S.A.* **96,** 11277–11282
41. Lin, J. T., Kormanec, J., Wehner, F., Wielert-Badt, S., and Kinne, R. K. (1998) High-level expression of Na^+/D-glucose cotransporter (SGLT1) in a stably transfected Chinese hamster ovary cell line. *Biochim. Biophys. Acta* **1373**, 309–320
42. Butt, H. J., and Jaschke, M. (1995) Calculation of thermal noise in atomic force microscopy. *Nanotechnology* **6,** 1–7
43. Hutter, J. L., and Bechhoefer, J. (1993) Calibration of atomic-force microscope tips. *Rev. Sci. Instrum.* **64,** 1868–1873
44. Baumgartner, W., Hinterdorfer, P., and Schindler, H. (2000) Data analysis of interaction forces measured with the atomic force microscope. *Ultramicroscopy* **82,** 85–95
45. Evans, E., and Ritchie, K. (1999) Strength of a weak bond connecting flexible polymer chains. *Biophys. J.* **76,** 2439–2447
46. Bell, G. I. (1978) Models for the specific adhesion of cells to cells. *Science* **200,** 618–627
47. Evans, E., and Ritchie, K. (1997) Dynamic strength of molecular adhesion bonds. *Biophys. J.* **72,** 1541–1555
48. Wielert-Badt, S., Hinterdorfer, P., Gruber, H. J., Lin, J. T., Badt, D., Wimmer, B., Schindler, H., and Kinne, R. K. (2002) Single molecule recognition of protein binding epitopes in brush border membranes by force microscopy. *Biophys. J.* **82,** 2767–2774
49. Wielert-Badt, S., Lin, J. T., Lorenz, M., Fritz, S., and Kinne, R. K. (2000) Probing the conformation of the sugar transport inhibitor phlorizin by 2D-NMR, molecular dynamics studies, and pharmacophore analysis. *J. Med. Chem.* **43,** 1692–1698
50. Panayotova-Heiermann, M., Loo, D. D., Lostao, M. P., and Wright, E. M. (1994) Sodium/D-glucose cotransporter charge movements involve polar residues. *J. Biol. Chem.* **269,** 21016–21020
51. Panayotova-Heiermann, M., Eskandari, S., Turk, E., Zampighi, G. A., and Wright, E. M. (1997) Five transmembrane helices form the sugar pathway through the Na^+/glucose cotransporter. *J. Biol. Chem.* **272,** 20324–20327
52. Panayotova-Heiermann, M., Leung, D. W., Hirayama, B. A., and Wright, E. M. (1999) Purification and functional reconstitution of a truncated human Na^+/glucose cotransporter (SGLT1) expressed in *E. coli*. *FEBS Lett.* **459,** 386–390
53. Panayotova-Heiermann, M., Loo, D. D., Kong, C. T., Lever, J. E., and Wright, E. M. (1996) Sugar binding to Na^+/glucose cotransporters is determined by the carboxyl-terminal half of the protein. *J. Biol. Chem.* **271,** 10029–10034
54. Da Cruz, M. E., Kinne, R., and Lin, J. T. (1983) Temperature dependence of D-glucose transport in reconstituted liposomes. *Biochim. Biophys. Acta* **732,** 691–698
55. Zaccai, G. (2000) How soft is a protein? A protein dynamics force constant measured by neutron scattering. *Science* **288,** 1604–1607
56. Nestorovich, E. M., Karginov, V. A., Berezhkovskii, A. M., Parsegian, V. A., and Bezrukov, S. M. (2012) Kinetics and thermodynamics of binding reactions as exemplified by anthrax toxin channel blockage with a cationic cyclodextrin derivative. *Proc. Natl. Acad. Sci. U.S.A.* **109,** 18453–18458
57. Tyagi, N. K., Puntheeranurak, T., Raja, M., Kumar, A., Wimmer, B., Neundlinger, I., Gruber, H., Hinterdorfer, P., and Kinne, R. K. (2011) A biophysical glance at the outer surface of the membrane transporter SGLT1. *Biochim. Biophys. Acta* **1808,** 1–18
58. Puntheeranurak, T., Kinne, R. K., Gruber, H. J., and Hinterdorfer, P. (2008) Single-molecule AFM studies of substrate transport by using the sodium-glucose cotransporter SGLT1. *J. Korean Phys. Soc.* **52,** 1336–1340
59. Aronson, P. S. (1978) Energy-dependence of phlorizin binding to isolated renal microvillus membranes. Evidence concerning the mechanism of coupling between the electrochemical Na^+ gradient the sugar transport. *J. Membr. Biol.* **42,** 81–98
60. Hirayama, B. A., Loo, D. D., Díez-Sampedro, A., Leung, D. W., Meinild, A. K., Lai-Bing, M., Turk, E., and Wright, E. M. (2007) Sodium-dependent reorganization of the sugar-binding site of SGLT1. *Biochemistry* **46,** 13391–13406
61. Restrepo, D., and Kimmich, G. A. (1986) Phlorizin binding to isolated enterocytes: membrane potential and sodium dependence. *J. Membr. Biol.* **89,** 269–280
62. Kienberger, F., Pastushenko, V. P., Kada, G., Gruber, H. J., Riener, C., Schindler, H., and Hinterdorfer, P. (2000) Static and dynamical properties of single poly(ethylene glycol) molecules investigated by force spectroscopy. *Single Molecules* **1,** 123–128
63. Maitra, A., and Arya, G. (2011) Influence of pulling handles and device stiffness in single-molecule force spectroscopy. *Phys. Chem. Chem. Phys.* **13,** 1836–1842
64. Novakova, R., Homerova, D., Kinne, R. K., Kinne-Saffran, E., and Lin, J. T. (2001) Identification of a region critically involved in the interaction of phlorizin with the rabbit sodium-D-glucose cotransporter SGLT1. *J. Membr. Biol.* **184,** 55–60
65. Raja, M. M., and Kinne, R. K. (2005) Interaction of C-terminal loop 13 of sodium-glucose cotransporter SGLT1 with lipid bilayers. *Biochemistry* **44,** 9123–9129